

Linear analysis of cylindrical ITG instability using Multi-Water-bag gyrokinetic models

N. Besse¹, D. Coulette¹

¹ Institut Jean Lamour CNRS, Nancy, France

Physical model

The physical system under study (see e.g [1] or [2]) is a cylindrical plasma column, magnetized by an axis aligned constant magnetic field. Ion dynamics is described by the Vlasov gyrokinetic equation in the low larmor radius limit. Electrons are assumed "adiabatic". Closure is provided by the quasi-neutrality equation with polarization drift. Multi-Water-Bag (Figure 1) reduction consists in considering an ion parallel velocity distribution function of the form :

$$f(\mathbf{r}, v_{\parallel}, t) = \sum_{\substack{j=-N \\ j \neq 0}}^N A_j \mathcal{H}(v_j(\mathbf{r}, t) - v_{\parallel}) \quad (1)$$

where \mathcal{H} is the Heaviside function, $A_j (j = 1..N)$ are constant positive weights and $A_{-j} = -A_j$. Space and time variations of the distribution function thus occur only through variation of the scalar fields v_j , defining the contours of the so-called "Water-bags". Taking into account symmetries of the initial equilibrium, the contours are decomposed as a sum $v_j(\mathbf{r}, t) = V_j(r) + w_j(r, \theta, z, t)$ of respectively 0th and 1st order fields. The radial enveloppe of the (m, n) Fourier mode of the Liouville transformed perturbed electric potential $\psi_{m,n\omega} = \sqrt{rn_0} \phi_{m,n,\omega}$ is then solution of the generalized Sturm-Liouville problem :

$$\left[-\frac{d^2}{dr^2} + Q(\omega) \right] \psi_{m,n,\omega} = 0 \quad \text{with} \quad \begin{cases} Q(\omega) = B(r) + F(\omega) \\ B(r) = \left(\frac{m}{r}\right)^2 + \frac{1}{Z_e T_e(r)} + \frac{1}{4} (d_r \ln(rn_0))^2 + \frac{1}{2} d_r^2 \ln(rn_0) \\ F(\omega) = -\sum_j \frac{A_j n k_{\parallel} - \frac{m}{r} d_r V_j}{n_0 \omega - n k_{\parallel} V_j} = \sum_j \frac{\Gamma_j}{\omega - \alpha_j} \\ \psi(r_{min}) = \psi(r_{max}) = 0 \end{cases} \quad (2)$$

All quantities above have been normalized as in [2].

Discrete model

To solve (2), the radial domain is split in N_r uniform samples $[r_i, r_{i+1}]$ and the derivation operator discretized with a second order finite difference scheme. The related discrete problem

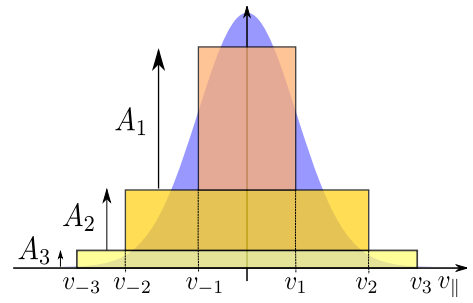


Figure 1: 3 bags MWB distribution and reference Maxwellian

is then :

$$[E(m, n, \omega)] [\psi(m, n, \omega)] = 0 \quad (3)$$

where $E(m, n, \omega)$ is an $(N_r - 2, N_r - 2)$ tridiagonal matrix, whose diagonal elements are rational functions of order $2N$ in ω .

Setting MWB parameters

Before actually solving (3), it is necessary to build an MWB distribution to match as closely as possible the initial physical situation. As MWB parameters do not have direct physical counter-parts, we require from the moments of the MWB distribution to equate those of a reference distribution, in our case a 0-centered Maxwellian, with prescribed density and temperature profiles. Symmetry then imposes $\forall j, V_{-j} = -V_j$, which leaves $2N$ unknowns to set. Moment equivalence with the p^{th} Maxwellian even moment μ_{2p} reads :

$$\sum_{j=1}^N \frac{2}{2p+1} A_j V_j(r)^{2p+1} = \mu_{2p}(r) \quad (4)$$

The contours are first either prescribed or computed by solving a generalized Hankel problem ([3]) at a reference radius r_0 . The weights A_j can then be computed by solving (4) for $0 \leq p \leq N - 1$. The contours values are then computed by Taylor expansion of (4) at second order and step-by-step extrapolation up to the domain borders. This procedure allows for a satisfying moment equivalence over the domain and accurate reproduction of parameters of interest, most notably the η_i radial profile.

Resolution strategies

The main difficulties in trying to solve problem (3) arise from the nonlinearity in ω , and the presence of the $2N \times (N_r - 2)$ poles $\alpha_j(r_i) = nk_{\parallel} V_j(r_i)$ on the real axis. Two main resolution schemes have been adopted :

- following a widely used procedure, the dispersion relation $\varepsilon(\omega)$ is obtained by computing the determinant of the matrix $E(\omega, m, n)$. As E is tridiagonal, $\varepsilon(\omega)$ and its derivative can be efficiently computed by a second order recurrence relation. The root of $\varepsilon(\omega)$ of highest imaginary part γ is then found by a classical subdivision scheme based on the argument principle in the complex plane. Once a root (ω_R, γ) is found, the relevant eigenvector is obtained by back-substituting the solution in $E(\omega)$ and singular value decomposition.
- a second approach consists in recasting problem (3) as a linear problem in the spectral parameter ω , i.e finding a pencil $A - \omega B = 0$ whose eigenstructure is the same. This can be done by going back to the continuous problem and defining a set of new unknowns

$g_j = \frac{\psi}{\omega - \alpha_j}$. Applying the same discretization scheme as before, one obtains for the $g_j(r_i)$ a pencil of size $(2N \times (N_r - 2), 2N \times (N_r - 2))$. The related generalized eigenvalue problem can then be solved readily by standard routines, and the full spectrum and eigenspace computed.

The main advantage of the first method is memory-compactness and speed if one only wants to compute the most unstable mode. The main draw-back is the sensitivity of the root-finding procedure when one approaches marginal stability, as the large density of poles on the real axis enhances integration costs. The ω -linearized problem allows for a more stable procedure and full eigenstructure solution, at the price of an increase in problem size. As a side note, the spectral linearization procedure can be applied to non-MWB and non-ITG models as long as they are formally equivalent to (2). For instance, we successfully reproduced results from [4] which deals with collisional drift-waves.

Some sample results

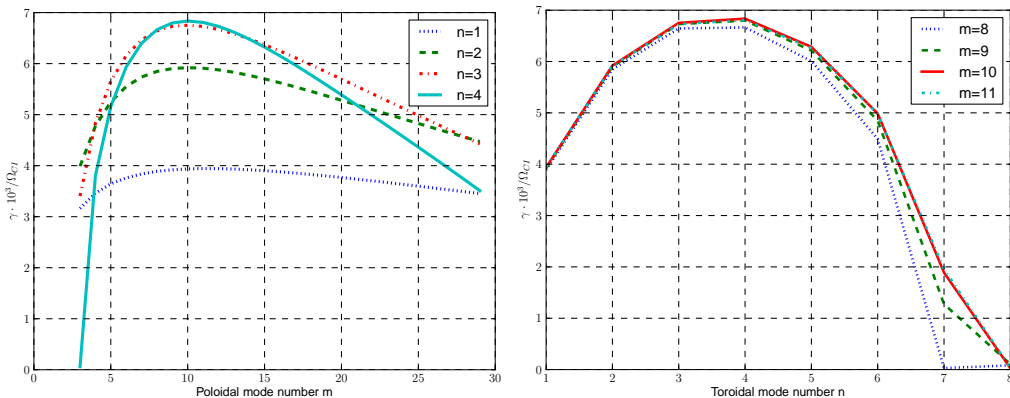


Figure 2: Evolution of growth rate with poloidal and toroidal mode numbers.

We present here results from a test case used in [2] to allow for comparison. Both equilibrium density and temperature profile exhibit a localized steep gradient at the reference position r_0 , providing a peaked η_i profile. An $N = 6$ MWB distribution was used. Growth rates (Figure 2) and frequencies are in good agreement with the KINEZERO kinetic code used in [2], which uses a real Gaussian ansatz for the radial dependency of the potential. Modulus of the radial envelope of the potential presents for the most unstable modes a skewed peaked profile, centered around the maximum of η_i . Localization and width of the mode is strongly dependent the value of the poloidal mode number m as can be seen in Figure 3. Phase variations of the eigenmodes, which could possibly lead to mode geometry distortion, are observed, but occur in radial zones where potential is extinguished, leading to no observable effect. It is possible to further observe the

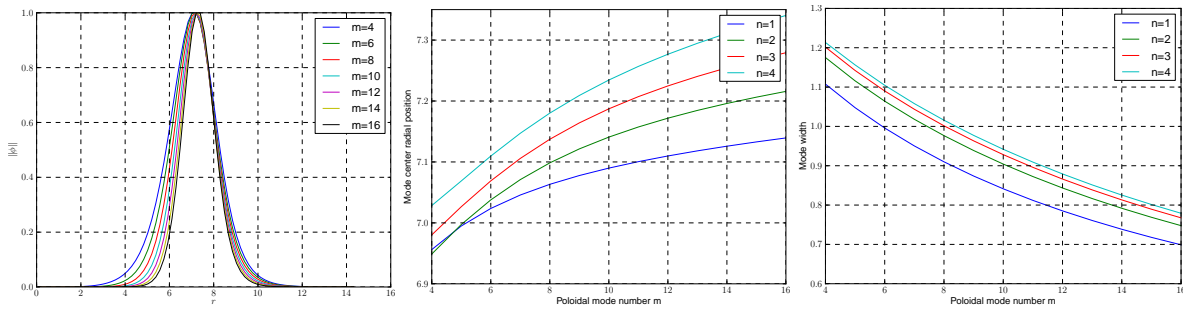


Figure 3: Evolution of mode structure with poloidal mode number

correlation between the most unstable mode over whole (m, n) domain and the η_i peak radial localization by moving the η_i peak position r_0 . In the table figure as can be expected the strong correlation between r_0 , r_{peak} and linear dependency with r_0 of the poloidal mode number of the most unstable mode.

r_0/ρ_s	3.5	5.3	7.2	9.0	10.8
n_{max}	4	4	4	4	4
m_{max}	5	7	10	13	15
r_{peak}/ρ_s	3.6	5.4	7.2	9.0	10.8
$\omega_R \times 10^3/\Omega_{CI}$	-13.2	-13.2	-13.2	-13.2	-13.2
$\gamma \times 10^3/\Omega_{CI}$	6.75	6.80	6.84	6.85	6.86

Figure 4: Effect of η_i localization on most unstable mode parameters

Conclusions and further work

The combination of MWB reduction and spectral linearization allows to obtain the full spectrum and eigenmodes of the instability with small computing costs (a few seconds for each (m, n) pair on a standard PC), while preserving accuracy. Non-local solving of (2) open the way for more thorough studies of spatial structures of linear modes, and provide relevant input data for quasilinear and nonlinear codes. Further work will focus on extending the methods to the toroidal ITG analysis and development of a new nonlinear cylindrical ITG code.

References

- [1] N. Besse and P. Bertrand. Gyro-water-bag approach in nonlinear gyrokinetic turbulence. *J Comput Phys*, **228** 3973-3995 (2009)
- [2] V. Grandgirard et al. A drift-kinetic Semi-Lagrangian 4D code for ion turbulence simulation. *J Comput Phys*, **217** (2) 395 - 423
- [3] B. Beckermann, G.H Golub, G.Labahn. On the numerical condition of a generalized Hankel eigenvalue problem. *Numer. Math* **106** 41 - 68 (2007)
- [4] R.F. Ellis and E. Marden-Marshall. Comparison of local and nonlocal theories of the collisional drift instability. *Phys. Fluids* **22** 2137 (1979)